

Princeton HEP 95-2
BELLE Note# 62
March 31, 1995

First Results from the BELLE DIRC Prototype

C. Lu, D. Marlow[†], C. Mindas, E. Prebys, W. Sands, & R. Wixted

*Joseph Henry Laboratories, Princeton University,
Princeton, NJ 08544*

Abstract

The DIRC (Detection of Internally Reflected Cerenkov light) is a new type of ring imaging Cerenkov detector, which detects images from Cerenkov light produced in precisely machined quartz bars. The Cerenkov images are transported along several meters of bar to the edge of the detector where they are proximity focussed unto an array of conventional photomultiplier tubes. Results from a prototype device comprising a $2 \times 4 \times 240$ cm³ quartz bar read by an array of 480 PMT's are presented. Sample images, which are the first observed in this type of detector, are shown. Measurements of the light yield (approximately 20 photoelectrons per image) and the angular resolution are in good agreement with Monte Carlo predictions.

[†] Corresponding author: E-mail MARLOW@PUPHEP.PRINCETON.EDU

1 Introduction

First proposed by Ratcliff and collaborators at SLAC[1, 2], the DIRC (**D**etection of **I**nternally **R**elected Čerenkov light) technique shows great promise as a particle ID system for e^+e^- B-Factory detectors. In particular, it promises $\geq 4\sigma \pi/K$ separation over the momentum range of interest, occupies only 5 – 10 cm of radial space inside of the calorimeter, and places a minimal amount of material (15%–20% r.l.) in front of the calorimeter. The DIRC has been considered for the PID systems of both the BaBar detector[3] at PEP-II and the BELLE detector[4, 5] at KEK.

The DIRC concept has been described in detail in references [1] & [2] and will be only briefly outlined here. The basic idea, shown in figure 1, is that a Čerenkov cone produced in a precisely machined rectangular quartz bar (typical dimensions $\sim 2 \times 4 \times 500 \text{ cm}^3$) will propagate by total internal reflection along the length bar to its end where it can be imaged by proximity focussing onto an array of conventional photomultipliers (more sophisticated focussing schemes are also possible, see reference [6]). If the surfaces of the bar are smooth and highly rectangular, the shape of the image can be readily calculated and provides direct information on the opening angle of the Čerenkov cone, and hence the particle's velocity.

In this note we summarize the experimental results obtained by the BELLE particle ID group. Measurements of bar quality, light yield, attenuation length, and single-photon resolution obtained from actual DIRC images of cosmic-ray muons obtained using BELLE's 480-PMT air-standoff prototype are presented.

2 Bar Quality

Although the dimensional tolerances and surface quality requirements are quite severe, it has been demonstrated that they are within the capability of the optics industry. In particular, the Zygo corporation of Middlefield, Connecticut[7], has produced several 120-cm-long bars of excellent quality that meet or exceed the DIRC's requirements.

One simple demonstration of bar quality was made using the 442 nm line from a 10-mW He-Cd laser. The profile of the beam was scanned by placing a 100- μm pinhole aperture in front of a PIN diode photodetector mounted on a micropositioner. Figure 2 shows the profile of the beam before and after a return trip along a 120-cm-long bar. The entrance angle of the laser was chosen such that the beam underwent approximately 100 internal side-wall bounces before detection. The resulting broadening of the beam is minimal, although there is a suggestion of a

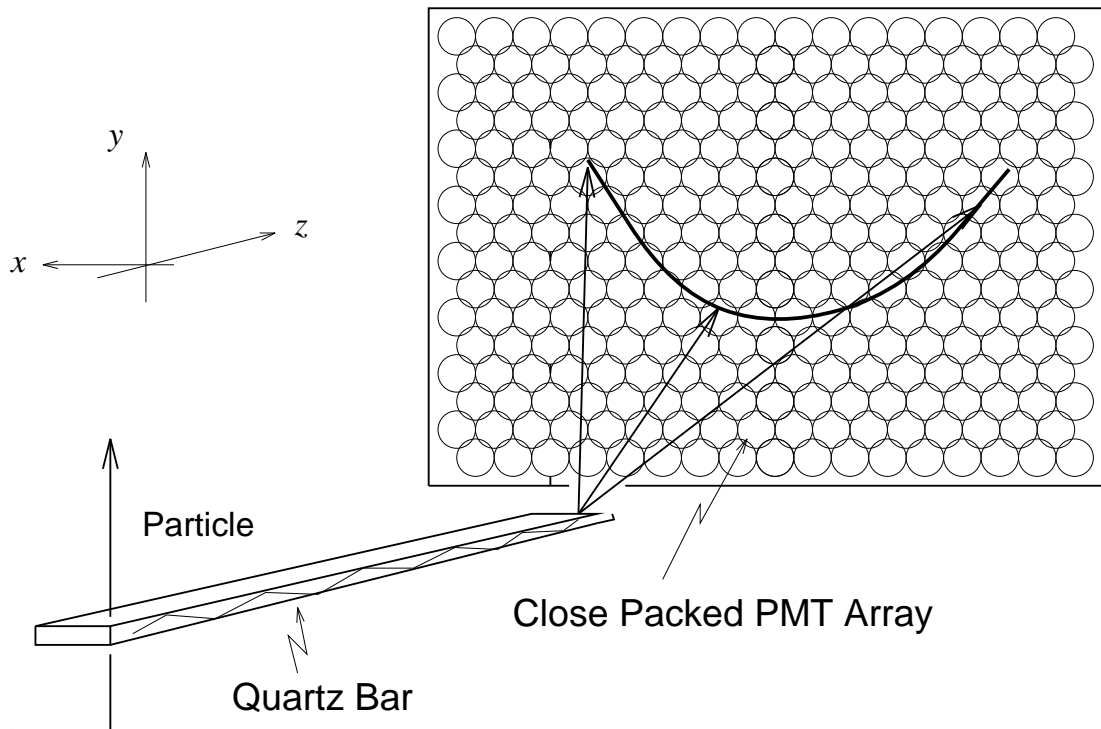


Figure 1: Principle of the DIRC. Čerenkov light from a particle crossing the bar propagates along the bar by total internal reflection to the end, where it emerges and is imaged onto a close-packed array of photomultipliers.

double peak, most likely the result of a corner reflection of the laser. However, the beam remains more than an order of magnitude smaller than the relevant size scale of a practical detector, which is set by the 30-to-40-mm diameter of the phototubes. Additional details on laser-based bar-quality measurements can be found in reference [8].

3 DIRC Prototype

The results to be presented here were obtained using a 480-PMT air-standoff DIRC, which is shown schematically in figure 3. Additional details can be found in reference [9]. Two 120-cm-long bars were glued together using Epotek 305 epoxy to form a single $2 \times 4 \times 240 \text{ cm}^3$ bar. A $15 \times 15 \text{ cm}^2$ horizontal mirror was placed at the readout end of the bar to deflect downward heading light emerging from the bar in the direction of the array. The face of a typical phototube in the array was situated 120 cm from the end of the bar. Although in a production device the standoff region (the volume between the quartz bar and the phototube array) will be filled with water, for this test, which was intended as a proof of principle, an air standoff was employed. This greatly simplified the engineering of the prototype.

The photodetector array comprised 480 38-mm-diameter 10-stage (Hamamatsu Model R580) PMT's mounted on ten separate HV-distribution/signal-collection printed-circuit boards. The PMT's were sorted by gain into groups of sixteen. Each such group shares a common HV divider string, substantially reducing the required number of HV channels and simplifying the assembly. The signals from the phototubes were readout using GASSIPLEX[10] chips developed at CERN for pad-chamber readouts. The GASSIPLEX chips were mounted in close proximity to the PMT's, which were coupled using a 5:1 capacitive divider. Although the 700 ns integration time of the GASSIPLEX chips would render them unsuitable for a production device (the inherent speed of the PMT's represents an important advantage for the DIRC), for cosmic-ray work, where the rate is low, it produces a convenient delay that eliminates the need for bulky trigger-delay cables. Moreover, the highly multiplexed nature of the GASSIPLEX allows us to read the entire array with a single CAMAC ADC module.

Cosmic-ray muons incident over an angular range $20^\circ < \theta_t < 30^\circ$ were selected using a three-scintillator telescope and a 40-cm-thick steel filter. The muons were tracked using a set of 6-mm-diameter straw chambers operating as drift chambers in limited streamer mode. These were arranged so as to provide two double-layer measurements in each view, thereby allowing measurements of θ_t and ϕ_t (the angles the muon makes with the vertical in the planes parallel to and normal to the bar's

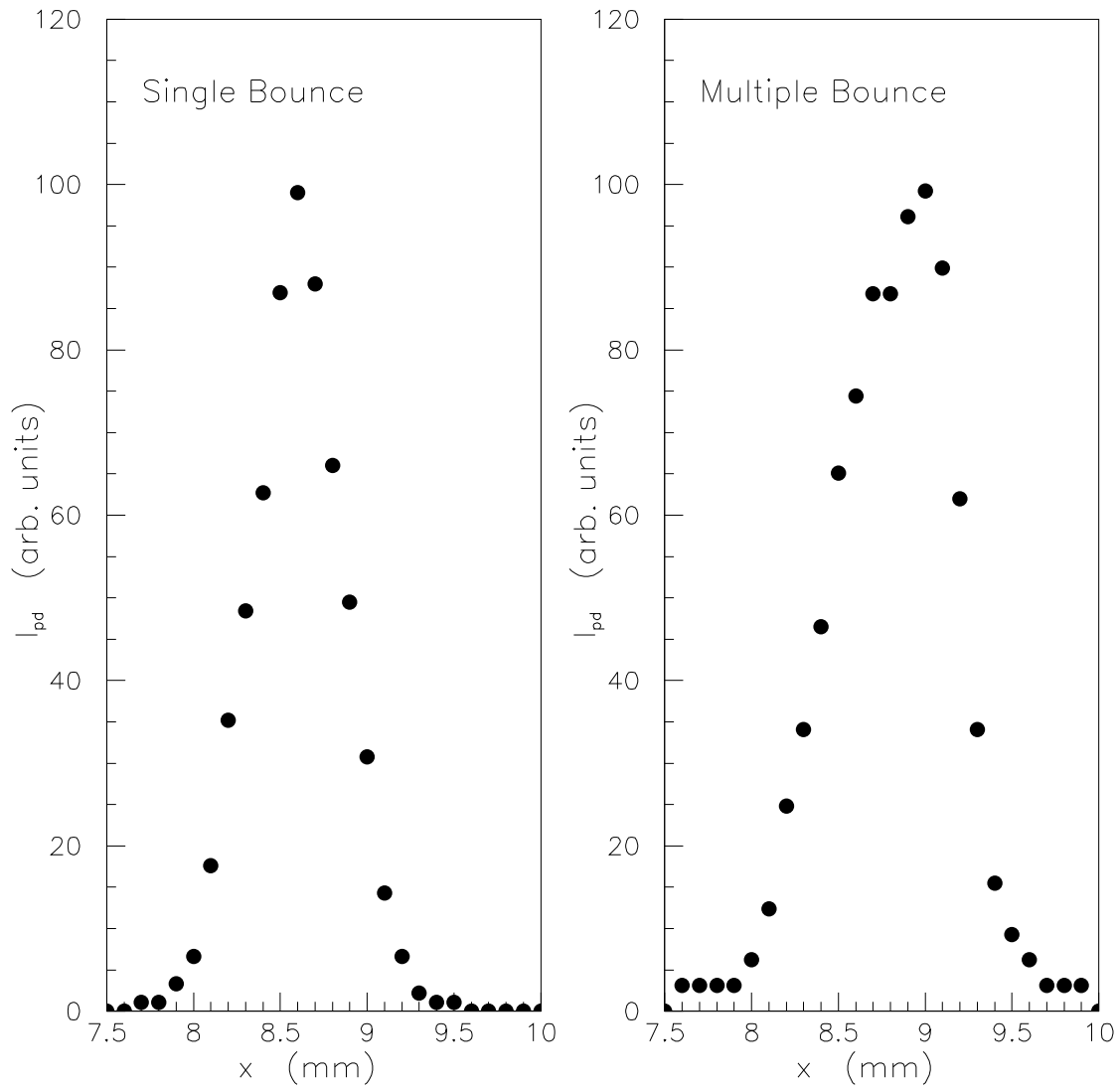


Figure 2: Beam profile of Čerenkov light. Left: beam profile after a single reflection. Right: beam profile after approximately 100 reflections.

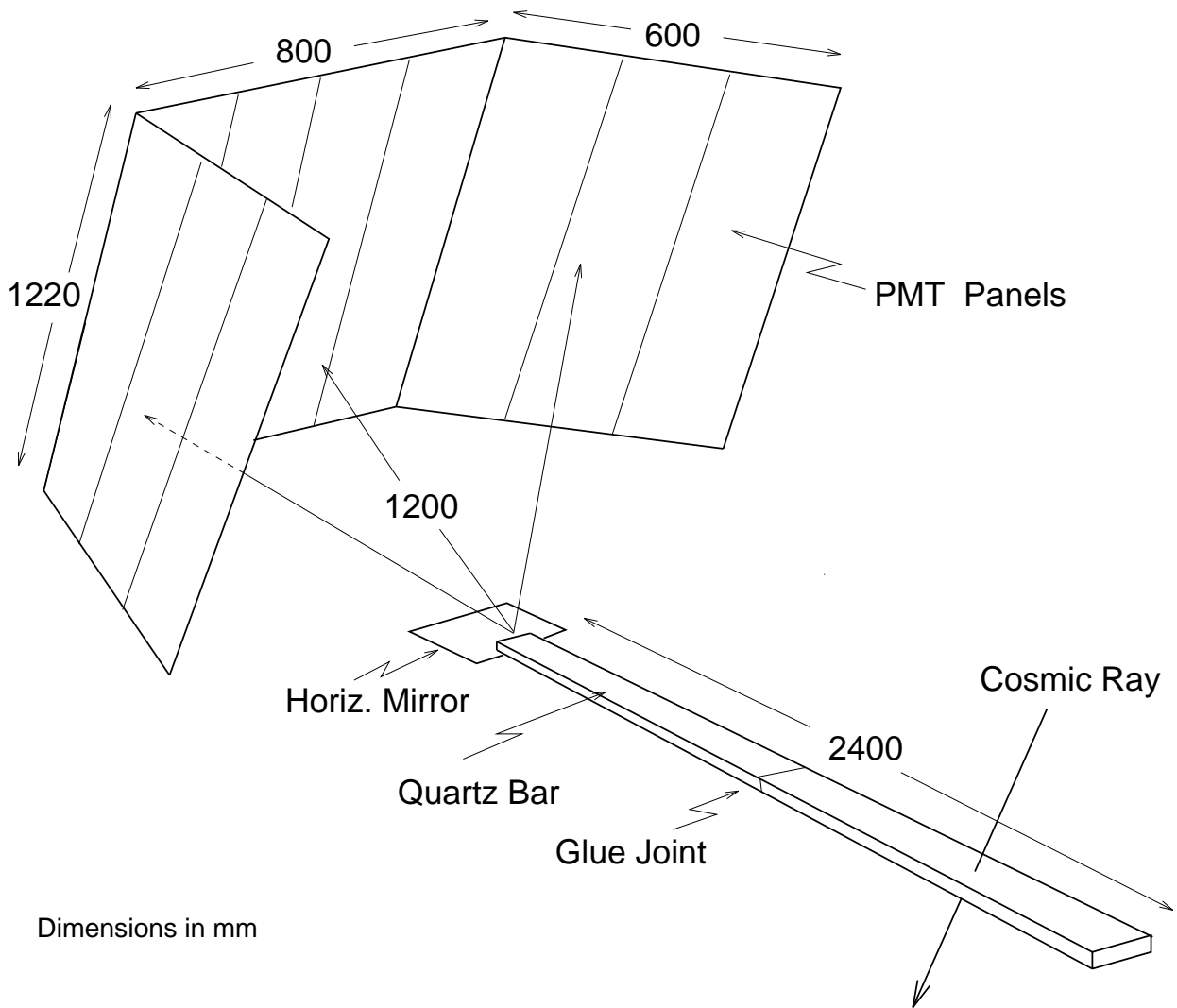


Figure 3: Perspective drawing of the BELLE DIRC prototype. The PMT's (not shown) are mounted on printed circuit boards that are attached to the vertical members of the PMT panels. The scintillator telescope used to select the cosmic rays is not shown.

axis, respectively) and completely determining the muons' incident trajectories.

The data reported here were taken in three sets of runs at three different locations along the bar. Two of the datasets were taken in “forward readout” mode—i.e. the angle of the telescope (25° to the vertical) was chosen so as to direct the Čerenkov light in the direction of the array. For these two datasets the distances between the telescope location and the readout end of the bar were 75 cm and 175 cm, referred to as “ $z = 75$ cm” and “ $z = 175$ cm,” respectively. For the third dataset, a “backward readout” mode was employed, wherein the orientation of the telescope was reversed (but kept at 25° to the vertical) such that the Čerenkov cone was directed initially away from the readout end of the bar. For this dataset, a mirror was placed at the end of the bar opposite from the readout to redirect the light back in the readout direction. Since the total distance (measured along the bar) covered by the light in this mode was approximately 410 cm, this data is referred to as the “ $z = 410$ cm” sample.

4 Results

The excellent performance of the DIRC is quite evident at a qualitative level from the four event displays shown in figures 4 and 5. These images were obtained within hours of turning on the array and are quite typical. The open circles show the positions of the phototubes if projected onto a flat plane coincident with the center panel. The solid circles represent struck phototubes and the open triangles represent struck phototubes with pulse heights that are small compared to the average for single photoelectrons but still above threshold.

The position and shape of the curves depend on the incident directions of the muons, which were determined by the straw chambers, and on the Čerenkov angle, which was taken as the single free parameter in a curve fitting position. Due to the left-right ambiguity in the reflection of the light (i.e., the number of horizontal bounces for a given photon can be either even or odd) there are in general two “solutions.” In cases where the incident muon is perfectly vertical, these two solutions coalesce, as is (nearly) the case in upper panel of figure 4 and the lower panel of figure 5.

In the sections that follow we present the results of a preliminary analysis of the quantitative aspects of the DIRC's performance.

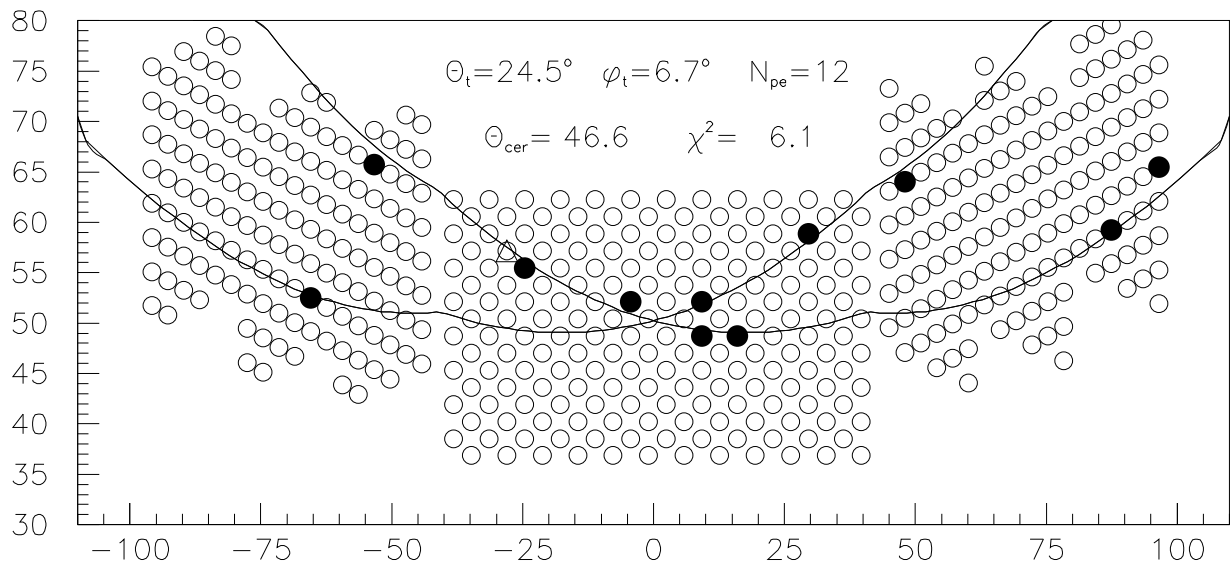
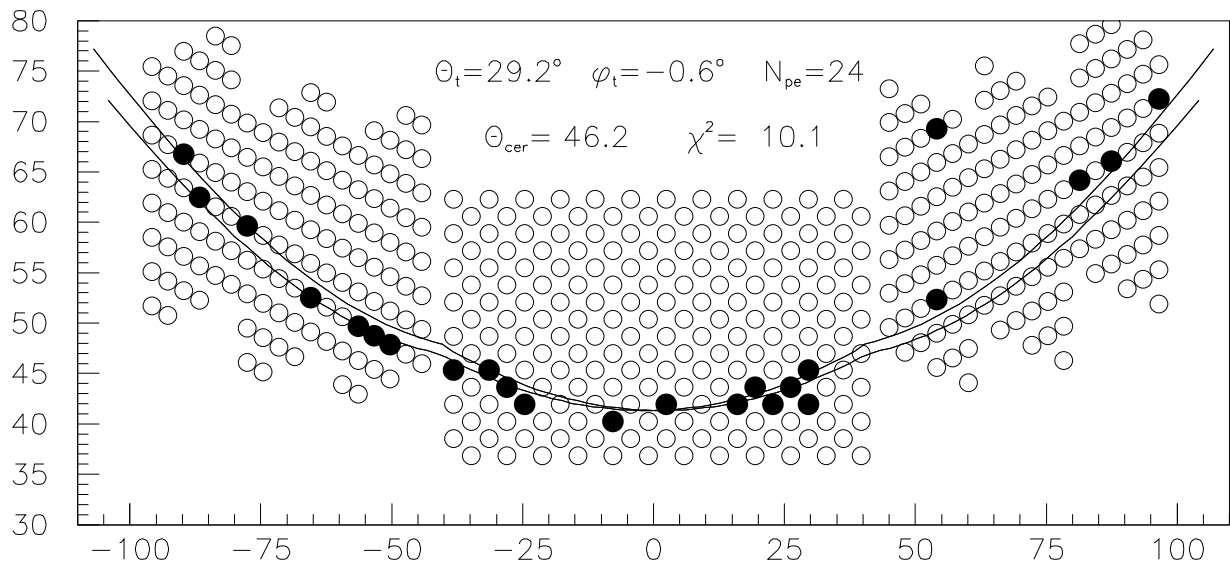


Figure 4: Two typical ring images.

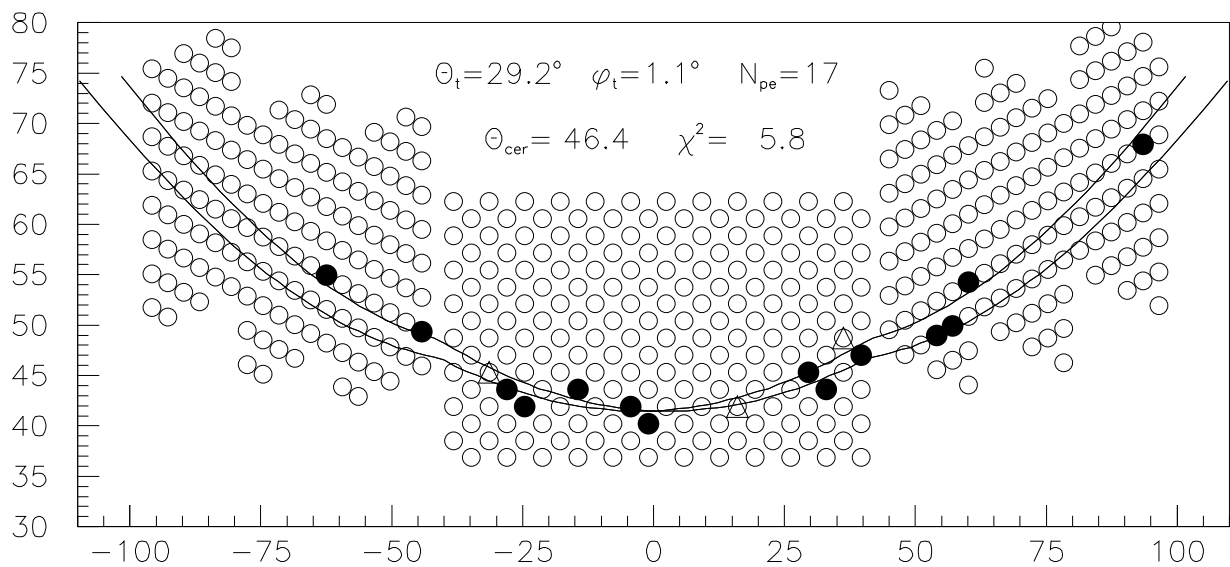
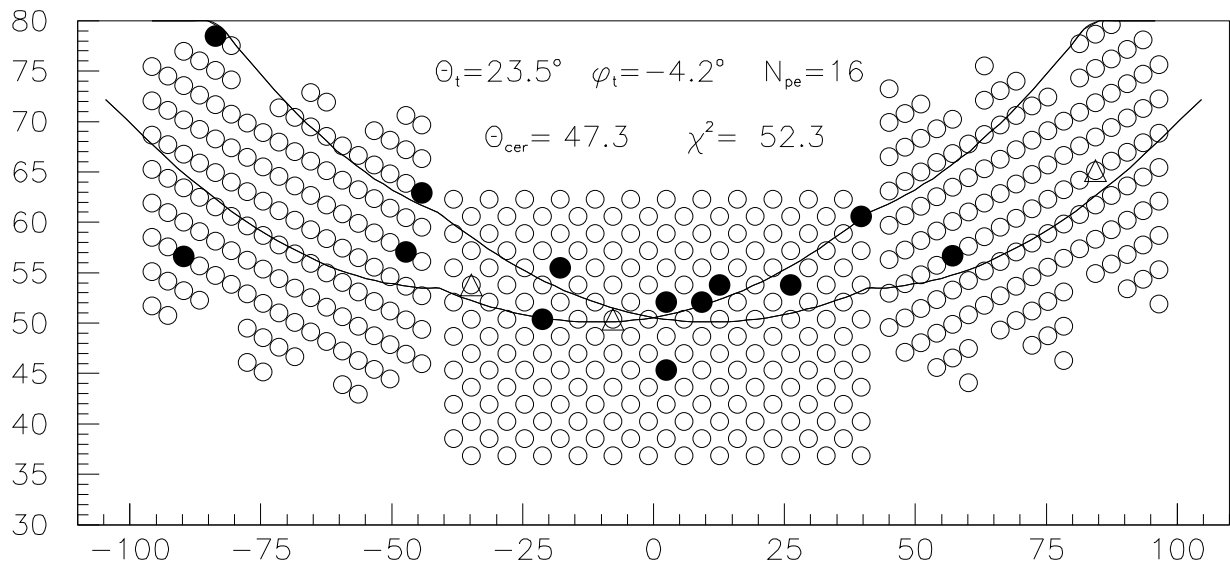


Figure 5: Two more typical ring images.

4.1 Photoelectron Yield

We first digress to summarize some basic notions regarding photoelectron yield calculations and some results obtained with a single PMT readout. A simple model for the light yield is

$$N_{\text{p.e.}}^{\text{obs}} = N_0 \langle \sin^2 \theta_C \rangle \varepsilon_{\text{geom}} \quad (1)$$

where $N_{\text{p.e.}}^{\text{obs}}$ is the observed (or predicted) photoelectron yield, $\langle \sin^2 \theta_C \rangle$ is a suitably averaged quantity determined mainly by the refractive index of the quartz, and $\varepsilon_{\text{geom}}$ is the geometric acceptance, which can be reliably calculated by Monte Carlo. The least certain factor is N_0 , the Čerenkov quality factor. In general N_0 depends on the quantum efficiency of the photocathode and on the transmission of the PMT window material (both functions of wavelength). Although in principle these quantities can be measured, a more practical approach is to determine N_0 by using the measured value of $N_{\text{p.e.}}^{\text{obs}}$ from a well understood geometry—i.e., a bar read at one end by a PMT.

Such a measurement was carried out using a Burle 8850 “Quantacon” PMT coupled to the bar with with $n = 1.40$ (GE Viscosil 600) grease. A yield of 66 ± 0.6 (stat) p.e.’s, was observed for a sample of hardened cosmic-ray muons incident at an average angle of $\theta = 30^\circ$ to the normal. This value was used to deduce $N_0 = 121$ p.e./cm. As a check, the measurement was repeated with air coupling to the bar, where Monte Carlo predicts the yield should be 50% of that for grease. The observed yield was 32.8 ± 1.7 (stat.) p.e. to be compared with the prediction of 33.4. The systematic error in the measurements is estimated to be 10%, due mainly to the systematic uncertainty in fitting the single photoelectron peak to determine the phototube gain and to uncertainties in the geometry of the cosmic-ray telescope. These measurements are in good agreement with previously reported results[11] and with results recently obtained in beam tests at KEK[12].

4.2 DIRC Prototype Yield Measurements

Figure 6 shows the photoelectron yield for the DIRC prototype operating using cosmic rays incident at 25° . The data include runs at both $z = 75$ cm and $z = 175$ cm (the yields are the same within statistics). The yield is defined as the number of PMT’s with ADC values that are 10σ above pedestal (pedestal widths are typically four ADC counts on a 10-bit scale)¹ The observed yield is $N_{\text{p.e.}} = 18.5 \pm 0.5$. The distribution is reasonably gaussian. Note that for the right-hand

¹We estimate that there is a 5-10% loss of photoelectrons due to this threshold, but we have not included it in our yield calculations.

plot in figure 6, the only cuts are on the straw tracking chambers. No requirements are placed on the DIRC array itself.

A Monte Carlo calculation of the expected yield using $N_0 = 121$ p.e./cm has been made. Including two approximately 4% losses due to Fresnel reflections at the quartz-air and air-PMT-window interfaces, the predicted yield is $N_{\text{p.e.}} = 18.5$. We estimate the systematic error to be approximately 10%. The close agreement between Monte Carlo and data is no-doubt fortuitous, but reassuring nonetheless. (Also, as discussed in section 4.2.1 below, the usable yield for these runs is actually 3%-6% lower.)

Figure 7 shows the photoelectron spectra for the $z = 410$ cm data. According to the vendor’s datasheets the broadband reflectivity of the end mirror is approximately 90% (the Fresnel reflections have little effect since they also direct the light back along the bar). Taking into account the additional path length along the bar of ~ 285 cm one expects an additional loss of about 15% from bar attenuation². Relative to the forward readout data we thus expect $N_{\text{p.e.}} \simeq 0.9 \times 0.85 \times 18.5 = 14$ for the backward readout. The observed value is $N_{\text{p.e.}} = 16.6 \pm 0.5$, somewhat higher than expected. We note, however, that the point-to-point systematics of these measurements are not well controlled (for example, the cosmic ray telescope must be completely disassembled each time the readout position is changed) and variations at the 10% level cannot be ruled out.

4.2.1 Single Photon Resolution

The Čerenkov angle resolution (or “ring” resolution) is approximately given by

$$\sigma_{\text{ring}} \simeq \frac{\sigma_{\gamma}}{\sqrt{N_{\text{p.e.}}}} \quad (2)$$

where σ_{γ} is the per-photon angular resolution and $N_{\text{p.e.}}$ is the yield. The main contributions to σ_{γ} come from chromaticity in the radiator and the spatial resolution of the photodetector. The latter is driven by the transverse dimensions of the bars, the size of the phototubes and the standoff distance. Both effects are included in the Monte Carlo. The spread in Čerenkov angles for muons passing through the bar and the steel range stack is estimated to be $\sigma_{\text{ring}}^{\text{cosmic}} \sim 5$ mrad. Since this is not negligible compared to the expected σ_{γ} , we have elected to plot a quantity called $\Delta\theta_C$, which is given by

$$\Delta\theta_C = \left| \frac{d\theta_C}{ds} \right| \Delta s \quad (3)$$

²This estimate is based on attenuation length measurements recently reported by Kichimi *et al.* at KEK, who report a good fit to their data assuming a surface reflectivity of $r = .9996 \pm .0003$

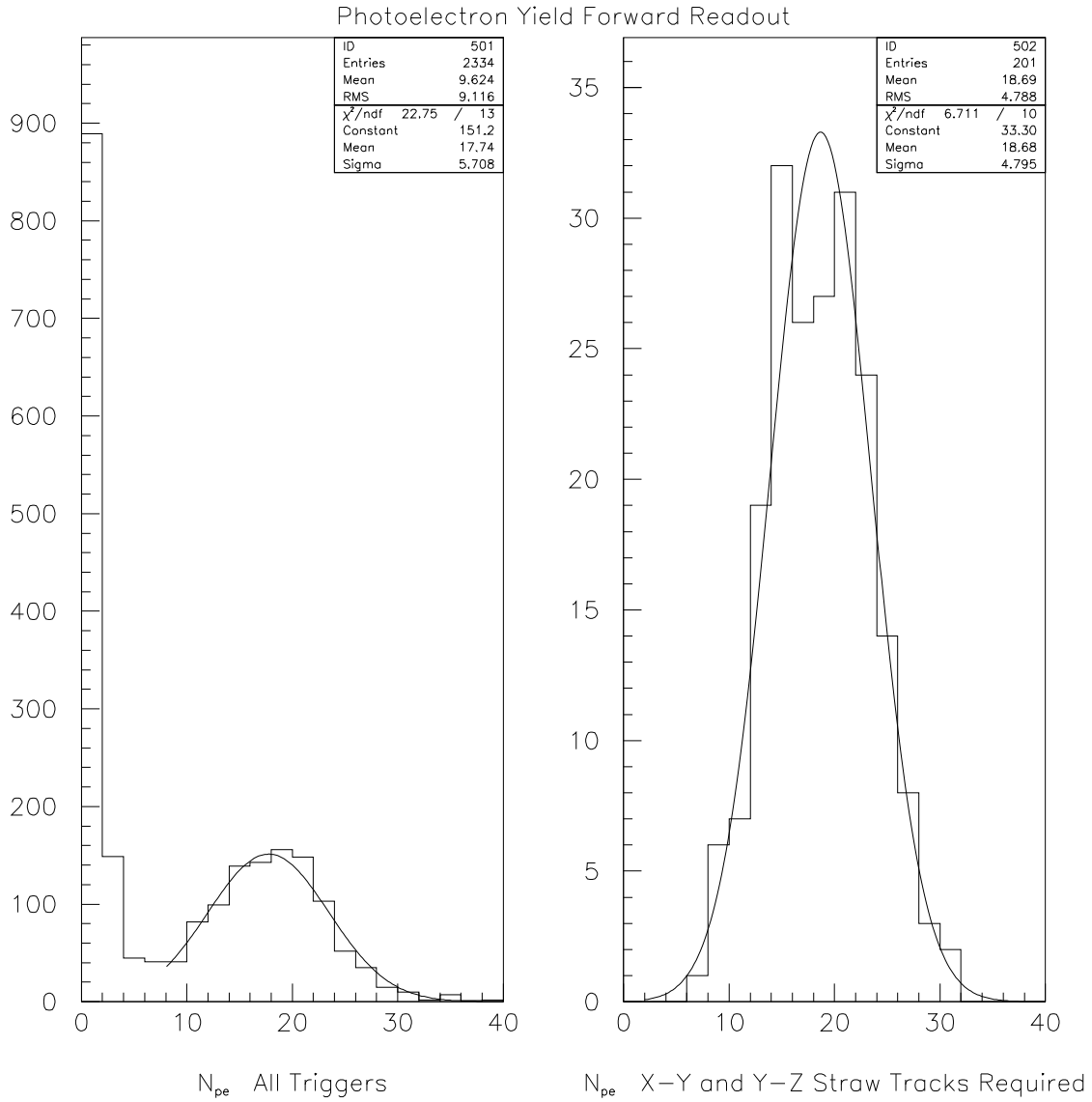


Figure 6: Photoelectron yield for the prototype array in forward readout mode. Left: number of struck PMT's for all triggers. Right: number of struck PMT's for triggers that result in straw-chamber tracks that pass through the bar. The data include runs from both $z = 75$ cm and $z = 175$ cm.

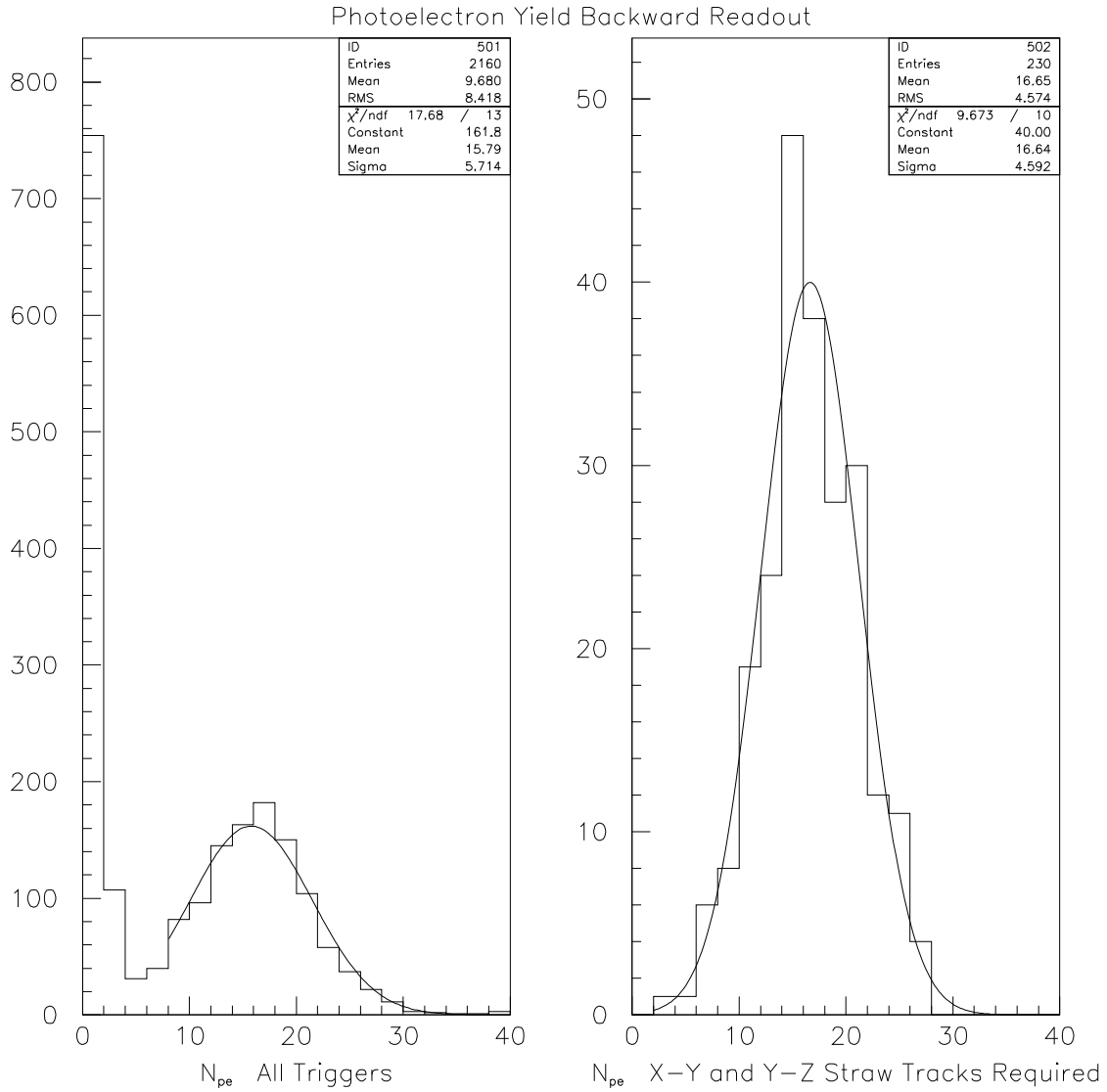


Figure 7: Photoelectron yield for the prototype array in backward readout mode. Left: number of struck PMT's for all triggers. Right: number of struck PMT's for triggers that result in straw-chamber tracks that pass through the bar. The data are from the $z = 410$ cm dataset.

where Δs is the distance of closest approach between the measured hit position and the fitted curve and $d\theta_C/ds$, which relates variations in Δs to changes in the Čerenkov angle, is calculated numerically for each photon. Note that since $\Delta\theta_C$ is in effect a fit residual, it strictly speaking is not the same as σ_γ . However, given that there are typically 15-20 photoelectrons per image, the two quantities should be reasonably close in value. In any event, since the same procedure is applied to both Monte Carlo and data it is possible to check for consistency.

Figure 8 shows the distribution of $\Delta\theta_C$ for the three datasets and for Monte Carlo. If a flat background term is added to the fits, the distributions are approximately, although by no means perfectly, described by single gaussians of $\sigma \simeq 9$ -10 mrad. Not surprisingly, the Monte Carlo distributions are more nearly gaussian with $\sigma = 8.6$ mrad—reasonable agreement given the maturity of the analysis.

There are some differences between data and Monte Carlo. First, there is a small, but statistically significant, difference in width between the width of the forward readout and backward readout datasets. The origin of this effect is under investigation, but is not currently known. The possibilities include dimensional imperfections in the quartz bars, performance variations in the cosmic-ray telescope (the angular resolution of the tracking chambers, for example, has an influence on the apparent photon resolution), and alignment of the forward mirror.

There is also a small uniform background whose magnitude appears to grow with distance.³ If one defines η_{bkg} as

$$\eta_{\text{bkg}} \equiv 1 - \frac{\# \text{ photons with } (-35 \text{ mrad} < \Delta\theta_C < 35 \text{ mrad})}{\text{total } \# \text{ photons}} \quad (4)$$

then $\eta_{\text{bkg}} = 3.6 \pm 0.6\%$, $4.9 \pm 0.4\%$, and $8.4 \pm 0.6\%$ (statistical errors) for the 75-, 175-, and 410-cm data, respectively. These hits are not predicted by the Monte Carlo, nor can they be attributed to solely to random backgrounds. From an analysis of pulser triggers the random background rate per event is 0.37 photons, which if the only source of background would result in $\eta_{\text{bkg}} \simeq 1.5\%$. Possible origins of the excess include small-angle scattering in the bulk quartz, surface imperfections, and scattering at the glue joint (this would not account for the $z = 75$ cm data). We note that since these photons do not contribute to the ring resolution, they should be subtracted from the yield numbers obtained in section 4.2 above.

³the ranges of the histograms in figure 8 correspond roughly to the size of the array, although there are a few events just outside of the displayed range.

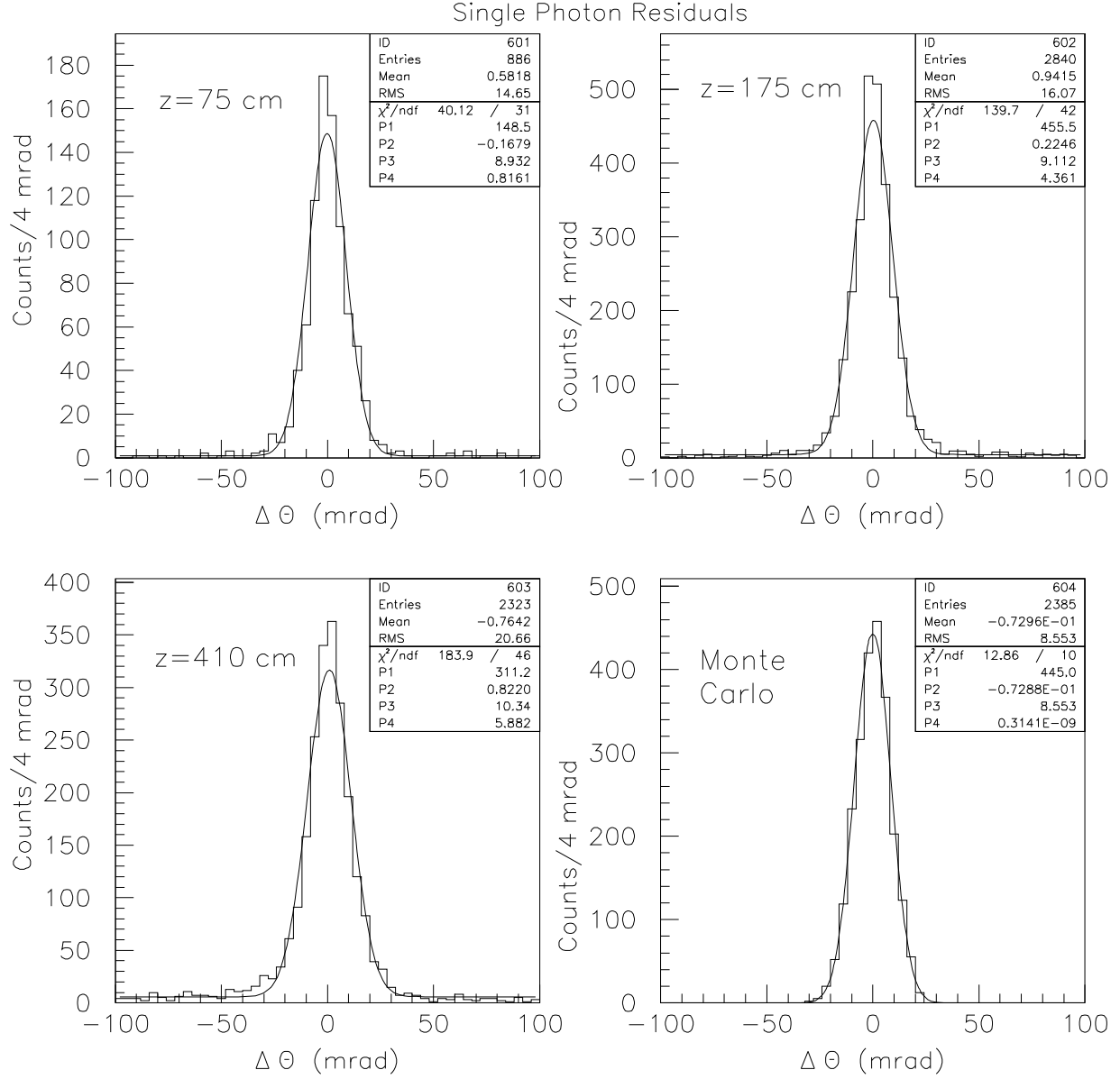


Figure 8: Distribution of $\Delta\theta_C$ for the various datasets and for Monte Carlo. The parameters P1, P2, and P3 correspond to the fitted amplitude, mean, and σ of the gaussian term. P4 is the amplitude of the flat background.

5 Summary and Conclusion

Preliminary test results from the BELLE DIRC prototype have been presented. The performance of the prototype is reasonably well described by the Monte Carlo, although there are some as-of-yet unresolved differences, which are currently under investigation. On balance, the performance of the device is remarkably good considering the early stage of development of DIRC technology.

6 Acknowledgements

We would like to thank F. Doss, T. Kamae, H. Kichimi, K. McDonald, S.K. Kim, Y. Sakai, F. Shoemaker, S. Uno and Y. Watanabe, for useful discussions and B. Ratcliff of SLAC, who was very generous in sharing his expertise and in lending us a quartz bar for our initial laser tests. K. Abe, S. Olsen, M. Selen, and F. Takasaki provided helpful advice and encouragement as well as material support in the form of phototubes and quartz bars. V. Polychronakis of BNL was kind enough to lend us the ADC readout module. Finally, we are also very grateful to C. Bopp, S. Chidzik, W. Groom, R. Klemmer, S. Morreale, A. Nelson, and R. Rabberman, for their excellent technical work.

References

- [1] B. Ratcliff, *Ba \bar{B} Collaboration Note #92* (Dec. 1992); P. Coyle *et al.*, SLAC Report SLAC-PUB-6371, (1993).
- [2] B. Ratcliff, "The DIRC Counter: A New Type of Particle Identification Device for B Factories," *Proceedings of the International Workshop on B-Factories: Accelerators and Experiments*, pg. 331, KEK Proceedings 93-7, (November 1992).
- [3] BaBar Detector Technical Design Report, March 1995.
- [4] "The DIRC Option for BELLE," , D. Marlow, BELLE Note 32, August 1994.
- [5] BELLE Detector Technical Design Report, KEK Report, January, 1995.
- [6] "Focussing DIRC as the Particle Identifier for the Forward End-Cap and Barrel Regions," T. Kamae *et al.*, BELLE Note 49, January 1995.
- [7] F. Doss, Zygo Corporation, Middlefield, Connecticut.

- [8] "Optical Tests of a Quartz DIRC Radiator Bar," C. Lu and D. Marlow, BELLE Note (in preparation).
- [9] "BELLE DIRC Phase I Prototype Notes," S. Kanda *et al.*, BELLE Note 39, November 1994.
- [10] The GASSIPLEX is a redesign of the AMPLEX chip by J.C.-Santiard of CERN. The original AMPLEX is described in E. Beuville *et al.*, Nucl. Inst. and Meth. A288 (1990) 157.
- [11] D. Aston *et al.*, talk by H. Kawahara at the IEEE 1994 Nucl. Sci. Symp., Norfolk VA, October 1994 (SLAC-PUB-6731).
- [12] H. Kichimi, private communication.
- [13] PEP-II Collaboration Letter of Intent, June 1994.